



Contents lists available at ScienceDirect



Catalysis Today

journal homepage: www.elsevier.com/locate/cattod

Alkylation of toluene with ethanol to *para*-ethyltoluene over MFI zeolites: Comparative study and kinetic modeling

Babatunde A. Ogunbadejo, Mogahid S. Osman, Palani Arudra, Abdullah M. Aitani,
Sulaiman S. Al-Khattaf*

Center of Research Excellence in Petroleum Refining & Petrochemicals, King Fahd University of Petroleum & Minerals, Dhahran 31261, Saudi Arabia

ARTICLE INFO

Article history:

Received 4 June 2014

Received in revised form 10 August 2014

Accepted 18 August 2014

Available online xxx

Keywords:

MFI

Crystal size

Para-selectivity

Para-ethyltoluene

Toluene ethylation

Ethanol

ABSTRACT

The production of *para*-ethyltoluene (*p*-ET) from the alkylation of toluene with ethanol was investigated over three MFI zeolites with varying $\text{SiO}_2/\text{Al}_2\text{O}_3$ ratio (80, 280, and 2000). The ethylation reaction was conducted in a batch fluidized-bed reactor at a temperature range of 300–400 °C, reaction times of 5–20 s and molar feed ratio of toluene to ethanol at 1:1. Toluene conversion increased with temperature over all the MFI zeolites except for MFI-80, which showed a maximum conversion of 29% at 300 °C. The product distribution exhibited ethyltoluenes as major product with a maximum yield of 26% over MFI-80. At 400 °C, constant toluene conversion of 14% and 100% ethanol conversion, para-selectivity to *p*-ET was 100% over MFI-2000 compared with 27% and 48% over MFI-80 and MFI-280, respectively. The high para-selectivity over MFI-2000 is attributed to the combined effects of higher $\text{SiO}_2/\text{Al}_2\text{O}_3$ ratio, very weak acid sites and larger crystal size (longer diffusion length). The experimental data were analyzed for each MFI zeolite and suitable reaction mechanism for toluene ethylation was proposed based on the Langmuir–Hinshelwood model. The activation energy for the formation of *p*-ET over MFI-280 and MFI-2000 is 30 kJ/mol and 65 kJ/mol, while the heat of adsorption of ethanol is 19 kJ/mol and 29 kJ/mol, respectively.

© 2014 Elsevier B.V. All rights reserved.

1. Introduction

The alkylation of toluene with ethanol produces ethyltoluenes which find applications in the petrochemical and chemical industries [1–5]. The ethylation of toluene with ethanol produces a wide range of hydrocarbon products which include C₁–C₄ gases (mostly obtained from dehydration and disproportionation reactions of ethanol and toluene, respectively), ethylbenzene, xylenes, and mixtures of ethyltoluene isomers [4–6]. In addition, other products such as styrene and methylstyrene could also be obtained as a result of side-chain alkylation, a condition favored by basic zeolites. The composition of the products may vary depending on the structural and morphological properties of the zeolites used [7–9].

Several researchers have investigated various parameters to enhance para-selectivity and catalyst activity. Parikh et al. studied the effects of crystal size and acidity on para-selectivity over A1-MFI

and B-, Fe-, Ga-isomorphously substituted zeolites of MFI structure with Si/metal ratios between 50 and 64 [10]. They reported that an increase in MFI crystal size results in a reduction in the active sites available on the external surface thereby inhibiting the isomerization of *p*-ET formed in the pores to other isomers. This is in conformity with the reaction mechanism proposed by Paparatto et al. using MFI ($\text{SiO}_2/\text{Al}_2\text{O}_3 = 25, 58, 63$) and MEL ($\text{SiO}_2/\text{Al}_2\text{O}_3 = 40, 80$). They concluded that *p*-ET is initially formed in the zeolite channels but undergoes isomerization if there are available acid sites on the external surface [8]. Wichterlova and Čejka [11] studied para-selectivity from the view point of the diffusion coefficient and coke deposition. It was observed that coke deposition did not influence para-selectivity, however, surface silylation with tetraethylorthosilicate (TEOS) could enhance *p*-ET due to pore narrowing.

Another important factor that could enhance para-selectivity is the external surface area. A correlation has been established between the crystal size and external surface area of MFI with $\text{SiO}_2/\text{Al}_2\text{O}_3$ ratios of 22 to 600 [11–14]. An increase in the crystal size translates to a reduction in the external surface which enhances the para-selectivity by impeding isomerization into meta and ortho isomers. Further improvement of para-selectivity over MFI can be

* Corresponding author. Tel.: +966 13 860 2029; fax: +966 13 860 4509.

E-mail addresses: ogunbadejo.babatunde@yahoo.com (B.A. Ogunbadejo), mogahid@kfupm.edu.sa (M.S. Osman), arpalya@kfupm.edu.sa (P. Arudra), aitani@kfupm.edu.sa (A.M. Aitani), skhattaf@kfupm.edu.sa (S.S. Al-Khattaf).

Nomenclature

C_i	concentration of specie i in the riser simulator (mol/m ³)
CL	confidence limit
E_i	apparent activation energy of the i th reaction (kJ/mol)
K_i	adsorption equilibrium constant of component i
k_i	apparent rate constant for the i th reaction (m ³ /kg of catalyst.s)
k_{oi}	pre-exponential factor for i th reaction after re-parameterization (m ³ /kg of catalyst s)
MW_i	molecular weight of specie i
R	universal gas constant (kJ/kmol K)
t	reaction time (s)
T	reaction temperature (K)
T_0	average temperature of the experiment (K)
V	volume of the riser (45 cm ³)
W_c	mass of the catalyst (0.81 g)
W_{hc}	total mass of the hydrocarbon injected the riser (0.162 g)
$\Delta S_{\text{ads},i}^0$	entropy for adsorption for componenet i
$\Delta H_{\text{ads},i}^0$	enthalpy for adsorption for componenet i
<i>Greek letters</i>	
φ	apparent deactivation function
α	catalyst deactivation constant (time on stream model)

achieved by impregnation of the zeolite channels with metal or non-metal oxides [15–18]. Modification of MFI (SiO₂/Al₂O₃ = 50) with different elements (B, P, Mg, Si, La, or Cd) showed an increase in para-selectivity to *p*-ET due to the decreased concentration of strong acid sites and the sorption capacity of the zeolite [16–19].

The heat of adsorption for toluene and ethanol was reported at 56 kJ/mol and 35 kJ/mol, respectively, with surface activation energy of 62 kJ/mol [16]. Parikh reported the kinetics of the ethylation reaction using a monolith reactor on which MFI (SiO₂/Al₂O₃ = 24) was wash-coated [20]. The proposed rate expression indicated that *p*-ET is the primary product of the alkylation reaction. *o*-ET was not considered due to negligible quantities while the net rate of *m*-ET formation was a result of the total rate of toluene consumption to form *p*-ET and the subsequent isomerization rate of *p*-ET to *m*-ET.

Most of the zeolites that showed high para-selectivity for toluene ethylation were subjected to post-synthesis steps either by modification of zeolite channels or deactivation of external surface. Consequently, the aim of this paper is to present aspects related to the development of a para-selective MFI-zeolite for toluene ethylation to *p*-ET without the need to modify either the zeolite pore channels or external surface. The paper addresses the effects of SiO₂/Al₂O₃ ratio, crystal size and reaction temperature on *p*-ET formation. It also focuses on development of a kinetic model accounting for all reaction steps i.e. adsorption, surface reaction and desorption.

2. Experimental

2.1. Materials

Two of the MFI zeolites used in this work were procured from Zeolyst; MFI-80 (CBV8014, NH₄-form) and MFI-280 (CBV28014, NH₄-form). Prior to catalyst testing, the zeolites were calcined

in standing air at 550 °C for 5 h (ramping rate of 3 °C min⁻¹), in order to get the H-form. MFI with a SiO₂/Al₂O₃ of 2000 (MFI-2000) was prepared using hydrothermal techniques, in a typical synthesis of this sample 4.26 g tetrapropylammonium bromide, 0.7407 g ammonium fluoride and hydrated aluminium nitrate 0.0750 was dissolved in 72 ml of water and stirred well for 15 min. 12 g silica (381276 Aldrich) was added and stirred well until homogenized. The obtained gel was autoclaved and kept at 200 °C for 2 days. The molar composition of gel was 1 SiO₂: 0.08 (TPA) Br: 0.10 NH₄F: 0.0005 Al₂O₃: 20 H₂O. The solid product obtained was washed with water and dried at 80 °C overnight. The template was removed by calcination in air at 750 °C for 5 h. These zeolites are hereafter referred as MFI-80, MFI-280 and MFI-2000, where the number represents the nominal SiO₂/Al₂O₃ ratio. Silicalite-1 was synthesized by the same procedure as MFI-2000 but without addition of aluminium source i.e. aluminium nitrate.

Toluene and ethanol were obtained from Sigma-Aldrich and no further attempt was made to purify the chemicals.

2.2. Catalyst characterization

The MFI zeolites were characterized using several techniques. The amounts of SiO₂ and Al₂O₃ the catalysts were determined by atomic absorption spectrometer (Perkin-Elmer AAS Analyst 100). Textural properties were characterized by N₂ adsorption-desorption measurements at 77 K, using Quantachrome Autosorb 1-C adsorption analyzer. Samples were outgassed at 220 °C under vacuum (10⁻⁵ Torr) for 3 h before N₂ physisorption. The Brunauer–Emmett–Teller (BET) specific surface areas were determined from the dsorption data in the relative pressure (P/P_0) range from 0.06–0.3, assuming 0.164 nm² for the cross-section of the N₂ molecule. Contribution of micropore and mesopores was derived from the *t*-plot method according to Lippens and de Boer [21].

High-angle X-ray diffraction patterns were recorded on a Rigaku Miniflex II XRD powder diffraction system using CuK α radiation ($\lambda_{K\alpha 1} = 1.54051 \text{ \AA}$, 30 kV and 15 mA). The XRD patterns were recorded in the static scanning mode from 1.2–60° (2 θ) at a detector angular speed of 2°/min and step size of 0.02°. The crystal sizes of the MFI zeolites were measured using a scanning electron microscopy (SEM) by Nova NanoSEM FEI with an accelerating voltage of 30 kV.

In order to assess the acid sites on the MFI zeolites and their properties, NH₃ temperature-programmed desorption (TPD) and FTIR spectroscopy of adsorbed pyridine were used. NH₃-TPD was carried out using Quantachrome Autosorb 1-C/TCD to determine total acid sites on the catalysts. Samples were pretreated at 450 °C in a stream of helium (25 ml min⁻¹) for 2 h. This was followed by the uptake of ammonia (5 vol. % in helium) at 100 °C for 30 min. The samples were then subjected to flow of helium for 2 h at 120 °C so as to remove loosely bound ammonia (i.e. physisorbed ammonia). After that, the samples were heated from 100–700 °C at a rate of 10 °C/min in a flow of helium (25 ml min⁻¹) while monitoring the evolved ammonia using TCD.

Infrared spectroscopy of adsorbed pyridine was used to identify the nature of available acid sites (i.e. Brønsted and/or Lewis acid sites). The measurements were conducted using a Fourier transform infrared with Nicolet FTIR spectrometer (Magna 500 model). The samples, as self-supporting wafers (ca. 60 mg in weight and 20 mm in diameter) were obtained by compressing a uniform layer of the powdered samples. The wafer was then inserted into an infrared vacuum cell equipped with KBr windows (Makuhari Rikagaku Garasu Inc., Japan), and preheated under vacuum (ca. 10⁻³ torr) at 450 °C for 2 h. The adsorption temperature of pyridine was 150 °C. The IR cell was then cooled down to ambient temperature and placed in an IR beam compartment while under vacuum

and transmission spectra were recorded. The bands and absorption coefficients used are as follows: pyridine (PyH^+) band at 1545 cm^{-1} , $\varepsilon = 0.078\text{ cm }\mu\text{mol}^{-1}$; pyridine (PyL) bands at 1461 and 1454 cm^{-1} , $\varepsilon = 0.165\text{ cm }\mu\text{mol}^{-1}$ [22,23].

2.3. Catalytic test

The ethylation of toluene with ethanol was conducted in a batch fluidized-bed reactor operated under atmospheric pressure. The reactor was designed to simulate an industrial scale reactor operated in batch mode with an impeller to aid gas mixing. The comprehensive description of the riser simulator can be found elsewhere [24].

The experiments for toluene ethylation with ethanol were performed using 0.81 g of catalyst with $1:1$ molar ratio of toluene and ethanol (equivalent to $67:33\text{ wt\%}$) at different reaction times of $5, 10, 15$ and 20 s and temperatures between 300 and 400°C . Before each experimental run, the catalyst was activated for 15 min at 610°C in a continuous flow of air after which the temperature was brought down to the desired reaction level. Once the reactor gets to the reaction temperature, the impeller was started with a speed of 5500 rpm and the feedstock was injected into the reactor via a pre-loaded syringe. At the end of the reaction, the port valve automatically opened ensuring termination of the reaction and the product was sent to an online gas chromatograph through the vacuum box. Each run was repeated to ensure the results can be reproduced with standard deviation in the range $\pm 2\%$. The response factor of each product was taken into account in analyzing the product distribution. The conversion, product yield, selectivity and para-selectivity were determined using the following relations:

$$\% \text{ toluene conversion} = \frac{\text{toluene in feed} - \text{toluene in product}}{\text{toluene in feed}} \times 100$$

$$\% \text{ yield}_i = \frac{\text{wt\% of product } i}{\text{wt\% of toluene in feed}} \times 100\%$$

$$\% \text{ selectivity} = \frac{\text{wt\% of ethyltoluenes (ET) in product}}{\text{wt\% of aromatics in product}} \times 100$$

$$\% \text{ para-selectivity} = \frac{\text{wt\% of } p\text{-ET in product}}{\text{wt\% of ET in product}} \times 100$$

2.4. Kinetic modeling

Phenomenological based kinetic model demonstrating the alkylation of toluene with ethanol is developed based on Scheme 1 and the observed data obtained from the fluidized-bed reactor at different reaction temperatures and varying reaction times. Isothermal reactor condition was assumed given that the amount of the reacting species is relatively small and the contribution of heat of reaction can be considered negligible.

Within the experimental conditions, the alkylation reactions were considered to be free from internal and external mass transfer limitations. This assumption is reasonable given the fact that the MFI sample used in this study has small crystallite sizes of $0.5\text{ }\mu\text{m}$ to

$2\text{ }\mu\text{m}$ [25]. For this crystal size range, one can expect that the value of the effectiveness factor should be close to one. Considering this fact, the effect of diffusion has not been incorporated in the kinetics analysis. Marin and co-workers reported the kinetic modeling of ethylbenzene dealkylation over Pt promoted MFI by neglecting the contribution of the diffusion resistance [26].

Langmuir–Hinshelwood mechanism with surface reaction control was proposed as descriptor of the kinetic of the reaction of toluene with ethanol. The proposed model considers only the adsorption of ethanol and ethyltoluenes on the catalyst sites, the adsorption of toluene and other products are negligible as compared to ethanol and ethyltoluenes. Ethanol has strong tendency to adsorb on catalysts site thereby transforming into surface ethoxy groups which further interacts with lightly adsorbed toluene to form ethyltoluenes [8]. According to the proposed reaction scheme, the rate of toluene disappearance and the rate of ethyltoluenes formation can be written as:

Rate of disappearance of toluene (T_0)

$$-\frac{V}{W_C} \frac{dC_{T_0}}{dt} = \left[\frac{k_1 K_{\text{EtOH}} K_{\text{EtTol}} C_{\text{EtOH}} C_{\text{EtTol}}}{(1 + K_{\text{EtOH}} C_{\text{EtOH}} + K_{\text{EtTol}} C_{\text{EtTol}})^2} \right] \varphi \quad (1)$$

Rate of ethyltoluenes formation (EtTol):

$$\frac{V}{W_C} \frac{dC_{\text{EtTol}}}{dt} = \left[\frac{k_1 K_{\text{EtOH}} K_{\text{EtTol}} C_{\text{EtOH}} C_{\text{EtTol}}}{(1 + K_{\text{EtOH}} C_{\text{EtOH}} + K_{\text{EtTol}} C_{\text{EtTol}})^2} \right] \varphi \quad (2)$$

where C_i is molar concentration of each species in the system, V is the volume of the reactor, W_C is the mass of the catalyst, t is time in seconds, φ is the apparent deactivation function, k_1 is the apparent rate coefficient and K_i is the adsorption coefficient of each species on the catalyst.

The reaction rate constant was represented with the temperature dependence using the following form of Arrhenius equation:

$$k = k_0 \exp \left(\frac{-E}{R} \left(\frac{1}{T} - \frac{1}{T_0} \right) \right) \quad (3)$$

where k_{10} is pre-exponential factor at the average temperature T_0 and E is apparent activation energy of the reaction.

The adsorption equilibrium constants with the temperature dependence can be expressed according to the following thermodynamic relations [27,28]:

$$K_i = \exp \left(\frac{\Delta S_{\text{ads},i}^0}{R} - \frac{\Delta H_{\text{ads},i}^0}{R} \left(\frac{1}{T} - \frac{1}{T_0} \right) \right) \quad (4)$$

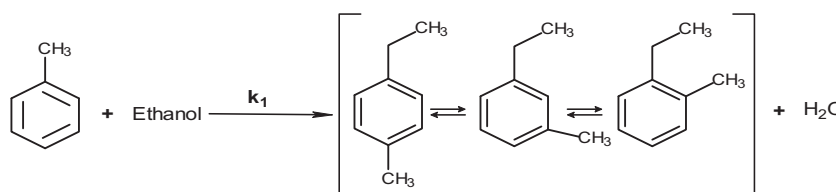
where $\Delta H_{\text{ads},i}^0$ is the change of enthalpy and $\Delta S_{\text{ads},i}^0$ is the change of entropy of the adsorption.

The effects of catalyst deactivation has been taken into account by considering a time on stream deactivation function as described in Eq. (5) [29].

$$\varphi = \exp(-\alpha t) \quad (5)$$

where, α is a constant and t is the time the catalyst is exposed to reaction.

A nonlinear regression algorithm (MATLAB, ODE 45-4th order Runge–Kutta method and least-square curve fitting “lsqcurvefit” routine) was used to solve the model equations and to obtain the



Scheme 1. Reaction network of toluene alkylation with ethanol.

Table 1

Physico-chemical properties of zeolite samples.

Zeolite sample	SiO ₂ /Al ₂ O ₃ ratio ^a	N ₂ sorption			
		d _{spacing} (Å) ^b	S _{BET} (m ² /g)	V (cm ³ /g) ^{c,d}	S _{meso} (m ² g ⁻¹) ^e
MFI-80	86	3.861	425	0.28 (0.19)	68
MFI-280	295	3.856	400	0.23 (0.21)	33
MFI-2000	2130	3.833	367	0.19 (0.18)	5.0
Silicalite-1	n.d.	3.824	363	0.19 (0.18)	3.0

^a AAS analysis.^b Evaluated by XRD (hkl = 501).^c Total pore volume.^d Number in parenthesis corresponds to micropore volume calculated using the t-plot.^e S_{meso} includes the mesoporous and external surface area, n.d. = not detected.

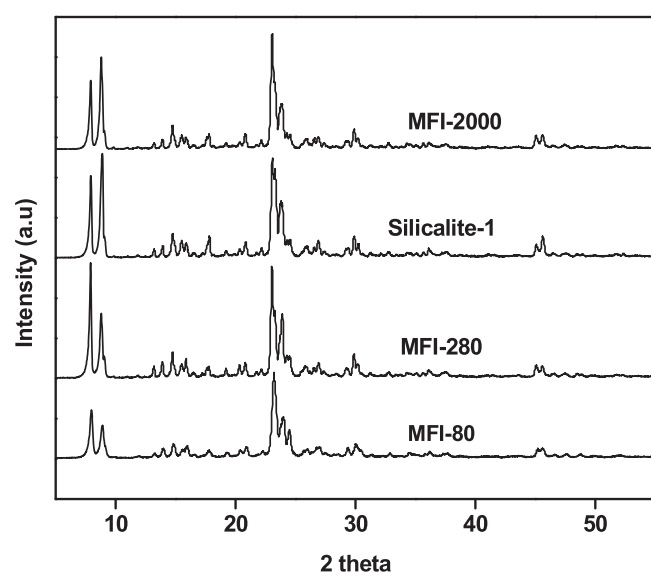
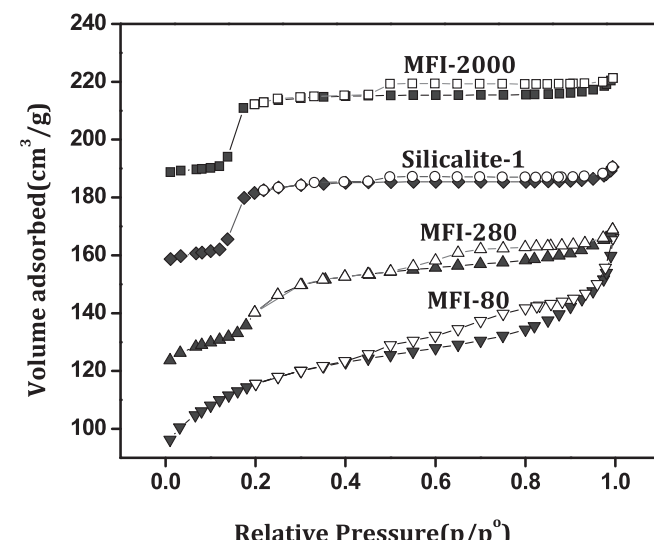
kinetic parameters. The optimization criteria for the model evaluation are that all the rate constants and the activation energies had to be positive and consistent with physical principles. The details of the regression analysis are described in Waziri et al. [30].

3. Results and discussion

3.1. Catalyst characterization

Table 1 shows the SiO₂/Al₂O₃ ratio for the MFI zeolites obtained by AAS analysis. The results show that MFI-80, MFI-280 and MFI-2000 have SiO₂/Al₂O₃ ratio of 86, 295 and 2130, respectively. The nitrogen adsorption isotherms results of the MFI zeolites and silicalite-1 are presented in Fig. 1. The textural parameters calculated from the nitrogen sorption isotherms are compiled in **Table 1**. The surface area of silicalite-1 is 363 m²/g, which is lower than that of other MFI zeolites. The incorporation Al atoms in the framework increased the pore volume as well as surface area of the material [31]. The total pore volume of MFI-2000 was similar to that of silicalite-1 due to the very low concentration of Al present in MFI-2000.

The XRD patterns of catalyst samples are presented in Fig. 2. The patterns of all samples exhibit XRD reflections that conform with the characteristic of MFI structure in the ranges between 8–9° and 22–25° [32,33]. The intensity of the peaks in the range 22–25° slightly decreased with an increase in SiO₂/Al₂O₃ ratio showing a slight decrease in crystallinity [34]. The values of lattice spacing d₅₀₁ determined by an XRD peak at (hkl) of 501 reflection are

**Fig. 2.** XRD patterns of MFI-80, MFI-280, MFI-2000 and silicalite-1.**Fig. 1.** N₂-adsorption–desorption isotherms of MFI-80, MFI-280, MFI-2000 and silicalite-1.

presented in **Table 1**. The values matched with standard MFI in the database [32].

The SEM micrographs of the three MFI zeolites are shown in **Fig. 3**. MFI-80 has a crystal size of about 0.5–1 μm and MFI-280 has 2–3 μm size, whereas MFI-2000 has a large crystal size of about 30–35 μm. The formation of uniform crystallite for MFI-2000 was also observed.

TPD profiles of desorbed ammonia for the three MFI are presented in **Fig. 4**. Two peaks appear in ammonia TPD profile for zeolites as reported by Kadota and Niwa [35]. They assigned the peaks appeared at a higher temperature and those appeared at a lower temperature to the ammonia desorbed from the acid sites of zeolites and ammonia molecules adsorbed either on NH₄⁺ species formed on Brønsted acid sites or on Na⁺ cations, respectively. In the present study, the numbers of acid sites were estimated from the areas of the peaks at a higher temperature and listed in **Table 2**. The number of acid sites increased with a decrease in SiO₂/Al₂O₃ ratio of MFI zeolites, which was expected. Pyridine adsorption by FT-IR spectroscopy was carried out to evaluate the strength and types of acid sites. **Table 2** presents the amount of Lewis and Brønsted acid sites in the MFI zeolites. For MFI-80 and MFI-280, the presence of both types of acid sites was observed, whereas in the case of MFI-2000 and silicalite-1 these sites were very weak and were not detected by FT-IR spectra recorded after the adsorption of pyridine and subsequent evacuation at 150 °C. The Lewis acid sites observed by IR of adsorbed pyridine are not the Na⁺ cations, but coordinatively unsaturated Al³⁺ cations formed by dehydroxylation of the OH groups bridging to Al and Si atoms (Brønsted acid sites).

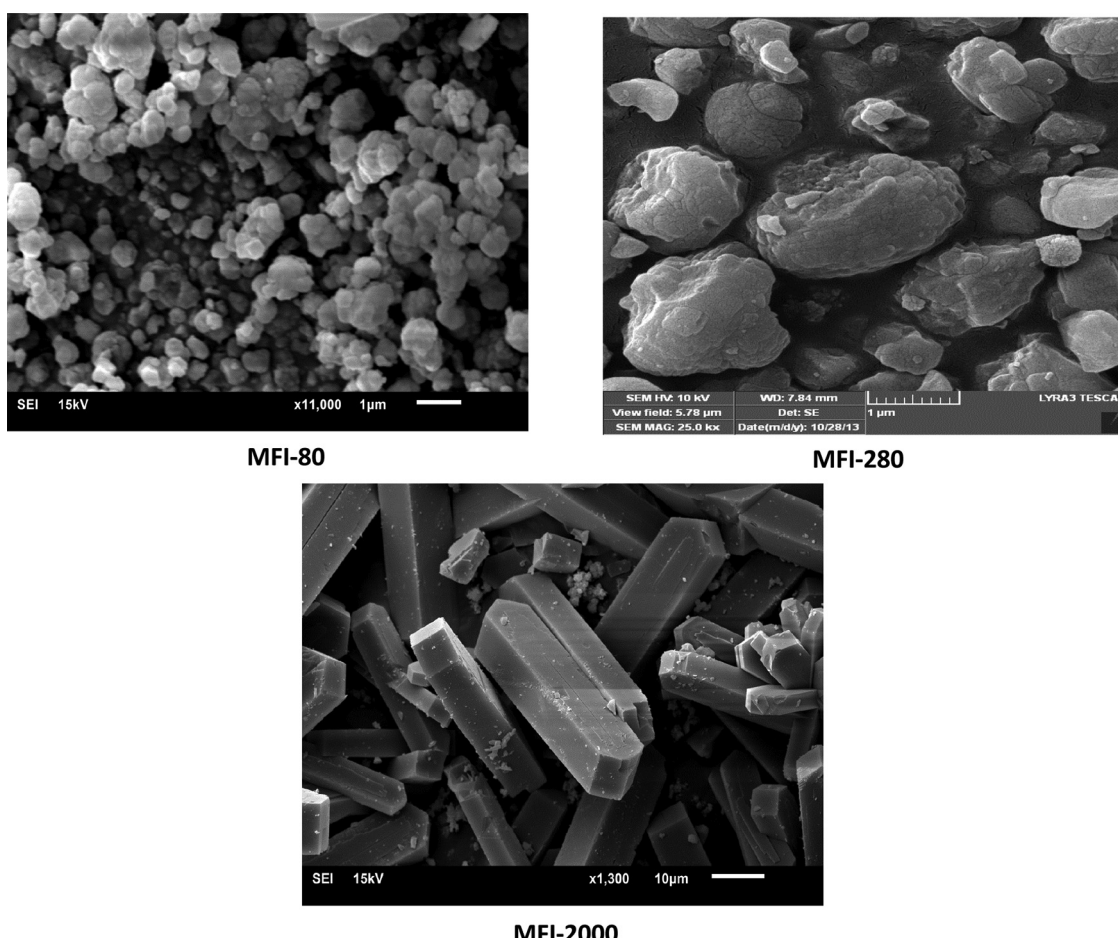


Fig. 3. SEM images of MFI-80, MFI-280, and MFI-2000.

3.2. Catalytic activity

Table 3 presents the catalytic performance of MFI zeolites for toluene ethylation with ethanol at different temperatures. The results comprise toluene conversion, product yields, selectivity to ethyltoluenes, *p*-ET, *m*-ET, and *o*-ET. In toluene ethylation over MFI-2000, it is evident that the major product at all temperatures studied was *p*-ET with trace amount of EB, xylene and benzene indicating a negligible degree of other side reactions such as disproportionation and dealkylation. This is attributed to the low acidity of the catalyst due to its low Al content [36]. The selective formation of *p*-ET over MFI-2000 may be attributed to the combined effect of acid sites, absence of external acid sites and crystal size. *p*-ET is formed within the zeolite pores being smaller in size than other isomers and its ease of diffusing over large crystal size in the range of 35–40 μm. The meta- and ortho-isomers are bulkier than *p*-ET and steric hindrance within the zeolitic pore could be expected. *p*-ET

undergoes isomerization to meta and ortho isomers at the external surface, subject to availability of Brønsted acid sites [8].

The formation of *m*-ET and *o*-ET isomers over MFI-280 was noticed at the reaction conditions studied. The product distribution over MFI-280 showed a higher quantity of disproportionation products than over MFI-2000. The production of diethylbenzenes (DEBs) over MFI-280 can be attributed to the availability of more Brønsted acid sites (**Table 2**). Over MFI-80, the product distribution became wider indicating significant presence of side reactions such as toluene disproportionation and isomerization yielding benzene, ethylbenzene, xylenes, DEBs and trimethylbenzenes (TMBs).

Ethanol conversion was much higher compared to toluene conversion at all temperatures although the same molar amount of ethanol and toluene was injected as feed. The main reason for higher ethanol conversion is attributed to the alkylation and dehydration reactions which consume the additional ethanol molecules.

Table 2

Acid sites characteristics and pyridine sorption data for zeolite samples.

Zeolite sample	NH ₃ -TPD (m mol g ⁻¹)			Pyridine FT-IR (m mol g ⁻¹) ^a		
	TA	L.T. < 300 °C	H.T. 300–550 °C	TA	B sites	L sites
MFI-80	0.16	0.09	0.07	0.14	0.08	0.06
MFI-280	0.07	0.05	0.02	0.02	0.01	0.01
MFI-2000	0.01	0.004	0.006	n.d.	n.d.	n.d.
Silicalite-1	n.d.	n.d.	n.d.	n.d.	n.d.	n.d.

^a Absorptivity ratio $\varepsilon_{1455}/\varepsilon_{1545} = 1.33$ was used to calculate the acidity; TA = total acidity; B = Brønsted acidity; L = Lewis acidity; nd = not detectable L.T. = low temperature; H.T. = high temperature; n.d. = not detected.

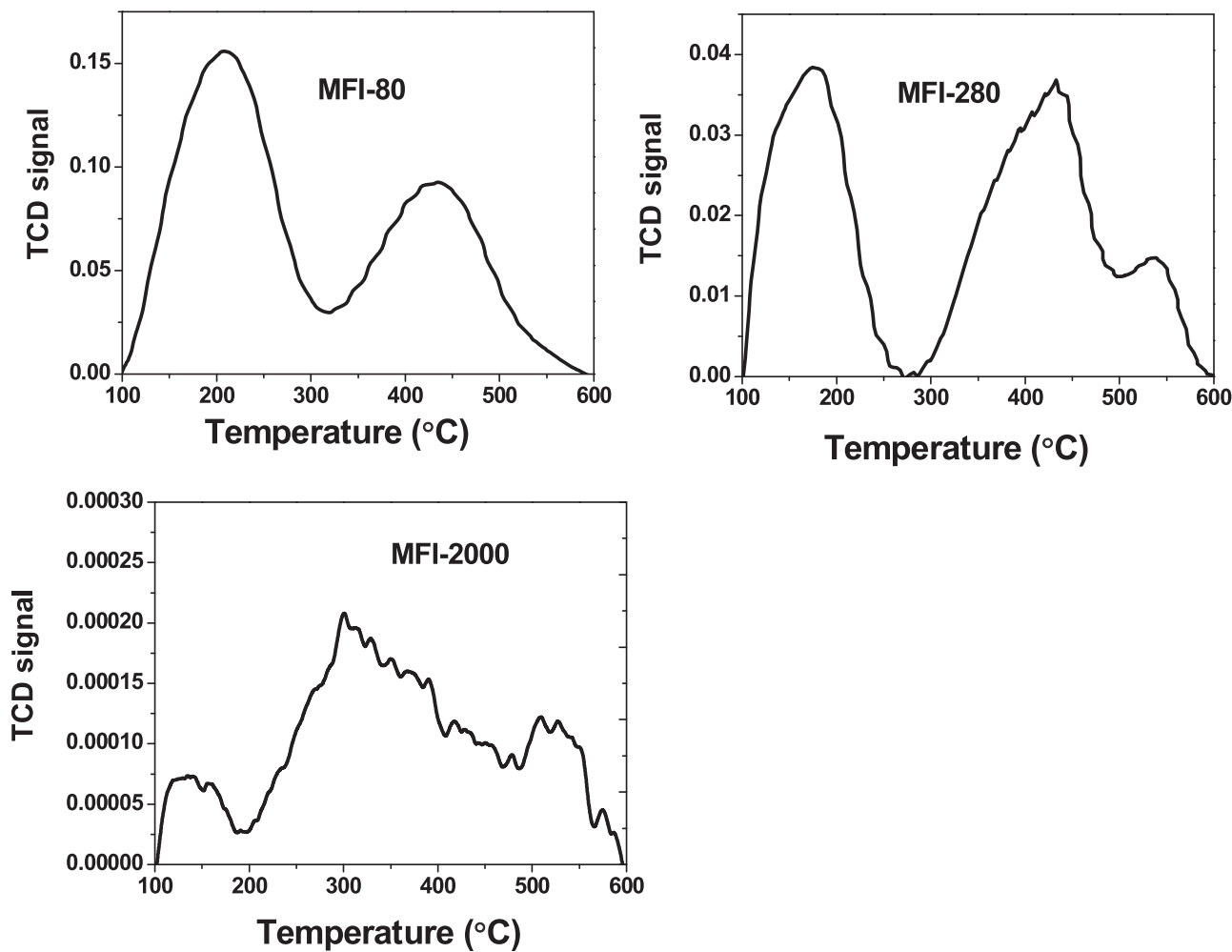


Fig. 4. TPD ammonia profiles of MFI-80, MFI-280 and MFI-2000.

The water molecules formed in alkylation of toluene by ethanol are adsorbed on Lewis acid sites to form protonic acid sites, and on the strong protonic acid sites to form hydronium ions which are weaker acid than the bridged OH groups. Therefore, water molecules might change the type of acid sites (Lewis acid to protonic acid) as well as weaken the protonic acid sites.

3.2.1. Effect of temperature

As shown in Fig. 5, there is an incremental increase in toluene conversion with the increase in temperature from 300 to 400 °C at 20 s reaction time for MFI-280 and MFI-2000 except that for MFI-80 which showed a reduction in toluene conversion from ~29% to ~22%. This drop in toluene conversion may be attributed to

Table 3

Catalytic performance of MFI-80, MFI-280 and MFI-2000 in toluene ethylation with ethanol at 20 s reaction time and 1:1 toluene:ethanol molar ratio.

Catalyst	MFI-80			MFI-280			MFI-2000		
	300	350	400	300	350	400	300	350	400
Toluene conversion (%)	29.0	29.0	22.2	18.6	22.3	23.8	1.5	8.0	14.2
Product yield (%)									
p-ET	7.3	6.3	3.6	9.4	11.2	8.5	1.5	7.7	13.5
m-ET	16.0	14.2	8.2	4.5	11.1	13.0	-	-	-
<i>o</i> -ET	2.8	3.2	2.1	-	0.3	1.0	-	-	-
Total-ET	26.1	23.7	13.9	13.1	22.6	22.5	1.5	7.7	13.5
Gases	3.9	4.5	7.4	2.5	2.3	2.1	10.8	8.8	7.9
Benzene	0.2	0.8	2.5	0	0	0.2	0	0.04	0.1
Ethylbenzene	0.9	1.5	1.8	0.3	0.6	0.9	0.03	0.1	0.3
Xylenes	0.9	2.0	3.36	0.1	0.5	1.1	0	0.2	0.3
DEBs + TMBs	0.9	0.9	0.7	0.6	0.4	0.3	0	0	0
ET selectivity (%)	90.0	82.0	64.7	92.9	93.8	90.0	98.0	95.8	95.0
ET composition (%)									
p-ET	27.8	26.4	25.9	67.6	49.6	37.8	100	100	100
m-ET	61.4	59.9	59.3	32.4	49.0	57.7	-	-	-
<i>o</i> -ET	10.8	13.7	14.8	-	1.4	4.5	-	-	-

DEBs = diethylbenzenes, TMBs = trimethylbenzenes.

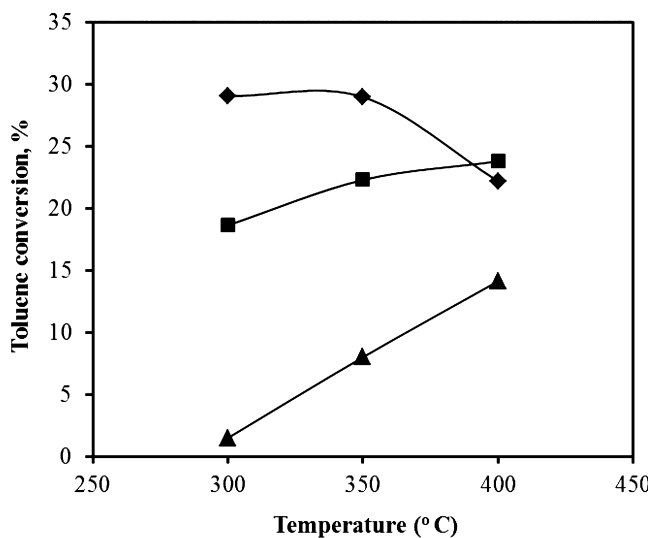


Fig. 5. Effect of temperature on toluene conversion over MFI-80 (♦), MFI-280 (■) and MFI-2000 (▲) at reaction time of 20 s.

coke formation which is accelerated by strong acid sites of MFI-80. Comparing MFI-80 and MFI-280 at 400 °C, the amount of C₁–C₄ gases for MFI-80 is 3 times more than that of MFI-280. Since these gases are produced from the decomposition of ethanol, it indicates that there is less amount of ethanol available for alkylating toluene to ethyltoluenes over MFI-80 as shown in Fig. 6(a) and Table 3. The formation of secondary alkylation products from toluene disproportionation or transalkylation with ET i.e. benzene, xylenes, EB, TMB and DEB over MFI-80 and MFI-280, means that some of the gases were consumed as methyl and ethyl groups. At 400 °C, the yield of ethyltoluenes over MFI-80 was 13.9% compared with 22.5% over MFI-280. A similar trend was also observed by Bhandarkar and Bhatia [17] over MFI ($\text{SiO}_2/\text{Al}_2\text{O}_3 = 50$) who attributed it to the decomposition of the alkylating agent and the possibility of reversible reaction within 300–400 °C. However, the increase in the yield of gases with the increase in reaction temperature over MFI-80, contrary to the behavior of MFI-280 and MFI-2000, may be attributed to the high amount of Brønsted acid sites in MFI-80 [37].

The yield of gases over MFI-2000 was the highest compared with MFI-80 and MFI-280. This may be attributed to the presence of weak acid sites in MFI-2000 which catalyze dehydration of ethanol but not so effective for isomerization of ET's (high p-ET selectivity) and disproportionation and transalkylation of toluene (low yields of benzene, xylene, EB, DEBs, TMBs). However, as the reaction temperature increased from 300 to 400 °C, the amount of C₁–C₄ gases produced over MFI-2000 dropped from 10.8% to 7.9%. This may be due to the partial consumption of these gases as shown in the product distribution in Table 3. Over MFI-2000, there was an increase in toluene conversion with the increase in temperature at different reaction times; however, the rapid increase was at a temperature of 400 °C. As the reaction time increased from 5 to 20 s, toluene conversion over MFI-2000 increased drastically especially at 400 °C as shown in Fig. 6(b). Maximum toluene conversion of 14% was obtained at 400 °C and a reaction time of 20 s.

3.2.2. Effect of $\text{SiO}_2/\text{Al}_2\text{O}_3$ ratio

The influence of $\text{SiO}_2/\text{Al}_2\text{O}_3$ ratio on the selectivity to p-ET over MFI zeolites is presented in Fig. 7 at 400 °C and constant toluene conversion of 14%. The para-selectivity to p-ET over MFI-2000 was 100% compared with 27% and 48% over MFI-80 and MFI-280, respectively. A similar trend was observed by Al-Khattaf and co-workers who studied the effect of $\text{SiO}_2/\text{Al}_2\text{O}_3$ ratio in

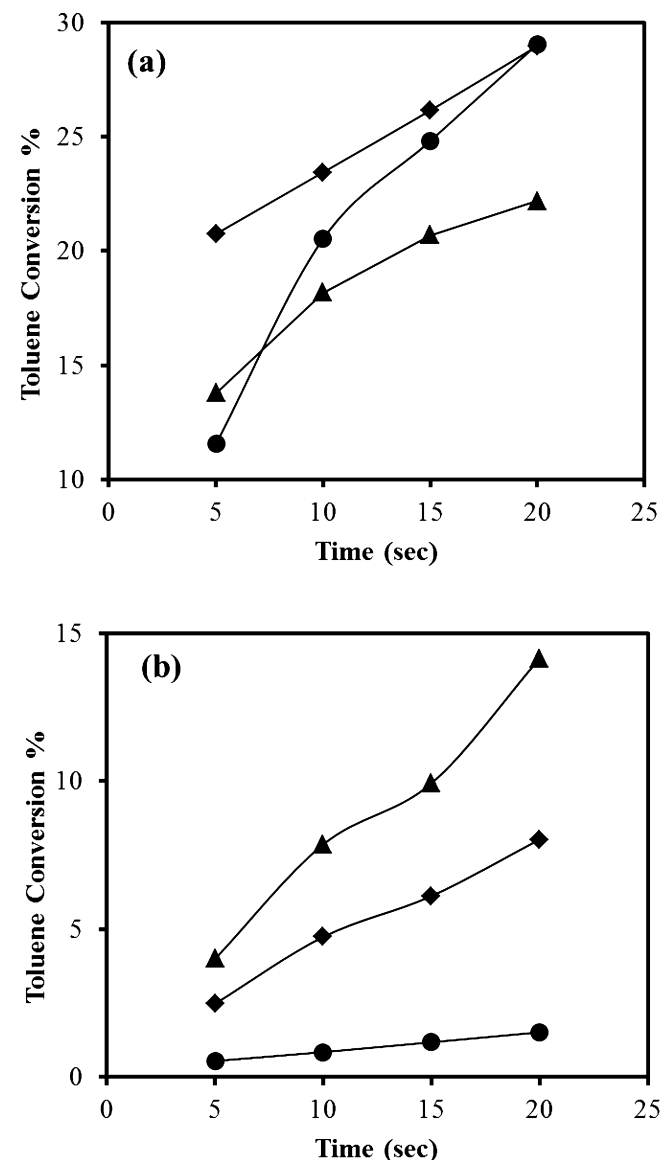


Fig. 6. Effect of reaction time on toluene conversion over (a) MFI-80 and (b) MFI-2000 at 300 °C (●), 350 °C (♦) and 400 °C (▲).

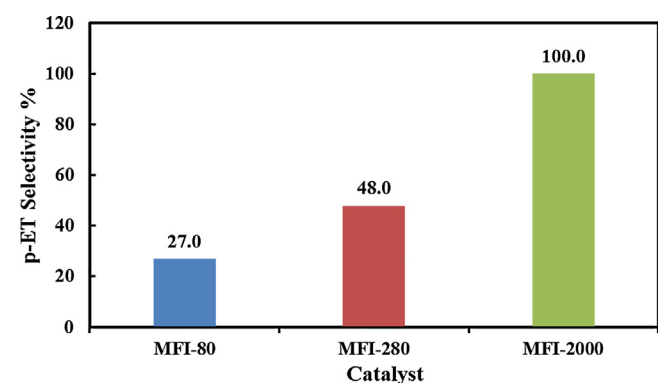


Fig. 7. *para*-Ethyltoluene selectivity over MFI-80, MFI-280 and MFI-2000 at 14% toluene conversion.

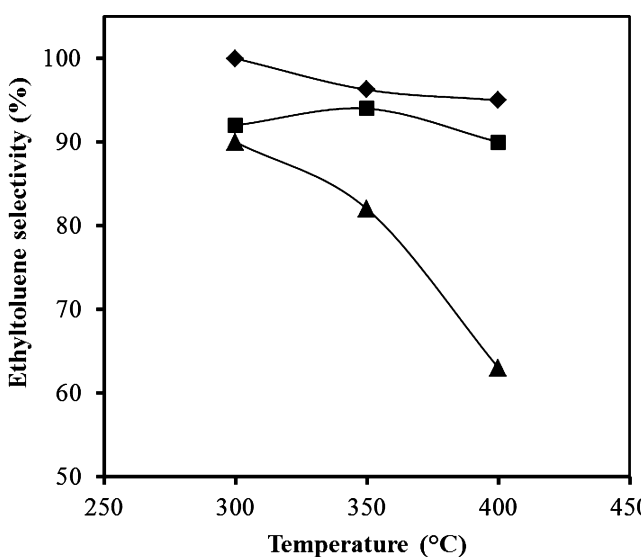


Fig. 8. Effect of temperature on ethyltoluenes selectivity over MFI-80 (▲), MFI-280 (■) and MFI-2000 (◆) at reaction time of 20 s.

diethylbenzenes synthesis over MFI and reported the same phenomenon for para-diethylbenzene selectivity [38].

It seems that irrespective of the reaction and product obtained over MFI zeolite, an optimum $\text{SiO}_2/\text{Al}_2\text{O}_3$ ratio generally favors para-selectivity [19]. Bhandarkar and Bhatia [17] obtained 56% para-selectivity at a toluene to ethanol ratio of 4:1 over MFI with $\text{SiO}_2/\text{Al}_2\text{O}_3$ of 50, whereas Paparatto et al. [9] reported 57% para-selectivity with similar feed ratio using MFI with $\text{SiO}_2/\text{Al}_2\text{O}_3$ of 25. The selectivities of the equilibrium mixture obtained over MFI-80 (*p*-ET 26.4%, *m*-ET 59.9%, *o*-ET 13.7%) were in agreement with those reported by Lee et al. over MFI with $\text{SiO}_2/\text{Al}_2\text{O}_3$ of 90 (*p*-ET 33.1%, *m*-ET 50.2%, *o*-ET 16.7%), keeping in mind that the conditions were slightly different [8].

For MFI-80 and MFI-2000, which have high and low concentration of acid sites, respectively, variation in temperature did not show any appreciable alteration to their para-selectivity. To elucidate the effect of $\text{SiO}_2/\text{Al}_2\text{O}_3$ ratio, silicalite-1 ($\text{SiO}_2/\text{Al}_2\text{O}_3 = \infty$) was tested for toluene ethylation. It was confirmed that neither activity nor selectivity was observed. At 300 °C and 20 s, toluene conversion was less than 0.4% and yield of ethyltoluenes was 0.2%. From the patterns observed over the three MFI zeolites, it is concluded that optimum $\text{SiO}_2/\text{Al}_2\text{O}_3$ ratio and large crystal size are necessary for maximum para-selectivity to *p*-ET. However, low $\text{SiO}_2/\text{Al}_2\text{O}_3$ ratio is required for high catalyst activity in the ethylation of toluene.

Fig. 8 presents the selectivity to ETs over the three MFI zeolites at different temperatures (300, 350, and 400 °C). The selectivity to ETs was observed to decrease with the increase in temperature for all zeolites associated with an increase in xylene, benzene and EB. The reduction in the selectivity to ET was most significant over MFI-80 in which the selectivity decreased from 90.0% to 64.7%. As shown in Fig. 8 and Table 3, the selectivity to ET over MFI-280 and MFI-2000 decreased by about 3% due to the formation of xylene and EB. The results obtained in our study is unique because the toluene to ethanol ratio used was 1:1 in contrast to what is reported in the literature, where high para-selectivity can only be achieved by using higher toluene to ethanol ratio.

3.2.3. Effect of crystal size

The high para-selectivity observed over MFI-2000 could also be attributed to its large crystal size of 30–35 μm [39]. Arsenova-Hartel et al. proposed an inverse relationship between the rate of isomerization and crystal size of the catalyst in their EB

Table 4

Estimated kinetic parameters for toluene ethylation over MFI-280 and MFI-2000.

Parameter	MFI-280	MFI-2000
k_{01} (m ³ /kgcat s)	0.32 ± 0.01	0.26 ± 0.01
E_i	30.2 ± 8.2	65.2 ± 9.3
$-\Delta H_{\text{ETOH}}$	19.1 ± 6.2	29.1 ± 5.1
$-\Delta H_{\text{ETTol}}$	32.7 ± 9.5	21.1 ± 4.2

disproportionation study over MFI [40]. They found that high content of p-DEB was noticed over large crystals than smaller ones due to the absence of diffusion limitation. Comparing the product distribution obtained over MFI zeolites, both MFI-80 and MFI-280 yielded appreciable amount of meta and ortho isomers due to their small crystal sizes (short diffusion length) meaning high active sites could be obtained on the external crystal surface. The absence of isomerization over MFI-2000 with higher crystal size gives strength to this assertion.

The effect of crystal size on toluene ethylation showed that the shape selectivity over MFI-zeolites falls under configurational diffusion-controlled selectivity. Chen et al. [41] explained that the differences between transition-state shape selectivity and configurational diffusion selectivity are the factors on which each of them depends, for configurational diffusion selectivity; it is affected by channel diameter and crystal size [42].

3.3. Kinetic model evaluation

Kinetic modeling of the toluene ethylation reaction has been developed based on Scheme 1 and the equations presented in Section 2.4. Langmuir–Hinshelwood model equations (Eq. (1) and (2)) incorporating the Arrhenius relation, the temperature dependence form of the equilibrium adsorption constants and deactivation function were simultaneously solved using a nonlinear regression analysis. The estimated kinetic parameters and their 95% confidence limits are shown in Table 4. The apparent activation energy (E) obtained from the regression analysis for toluene ethylation over MFI-2000 is more than double (65 kJ/mol) that of toluene ethylation over MFI-280 (30 kJ/mol). This may be attributed to both acidity and diffusion effects. The apparent rate constant for the MFI-2000 is smaller than that of MFI-280 due to the difference in external surface area. This has led to a lower activation energy for MFI-280 compared with MFI-2000 [43]. Furthermore, the acidity of

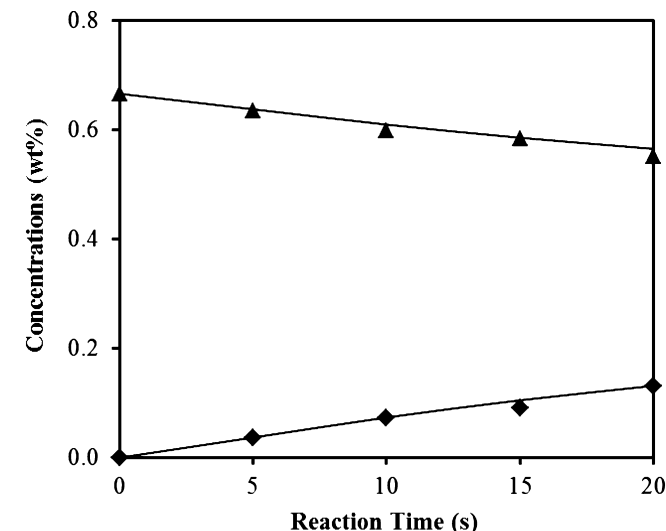


Fig. 9. Comparison between the experimental data (symbols) and predicted values (dotted lines) for the concentration of toluene (▲) and ethyltoluenes (◆) at 400 °C.

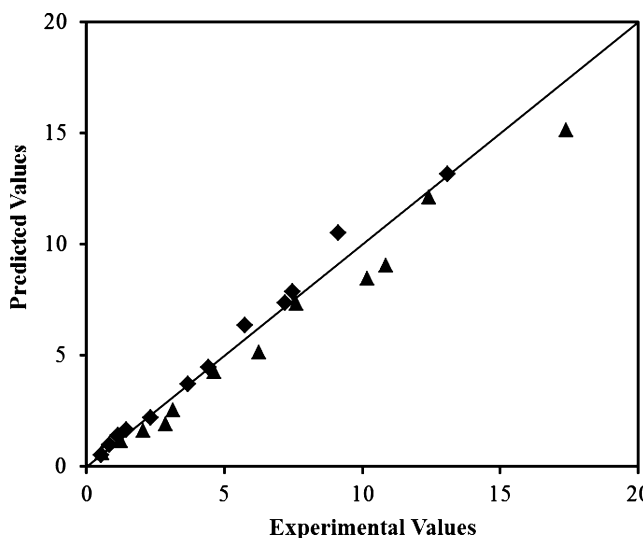


Fig. 10. Reconciliation plots between model predictions and experimental data. Experimental data: data points, model prediction: continuous line (toluene conversion % (▲), ethyltoluenes yield % (◆)).

MFI-280 is about seven times that of MFI-2000 which also led to a lower activation energy for MFI-280 compared with MFI-2000.

Al-Khattaf and co-workers showed similar trend for the activation energy of EB ethylation over MFI with varying $\text{SiO}_2/\text{Al}_2\text{O}_3$ ratio [38]. The estimated adsorption enthalpies for ethanol and ethyltoluenes are presented in Table 4. The results indicate a comparable adsorption strength over both MFI-2000 and MFI-280. Comparing the experimental data with the model predictions, it can be seen from Fig. 9 that toluene and ethyltoluenes concentrations predicted by the proposed model fit with the experimental data in an excellent manner. Toluene conversion and ethyltoluenes yields (Fig. 10), showed accurate match between experimental values and model predictions. The results of the kinetic study clearly show that MFI zeolites with different $\text{SiO}_2/\text{Al}_2\text{O}_3$ ratios have a significant impact on the mechanism of toluene ethylation with ethanol.

4. Conclusion

The ethylation of toluene with ethanol over MFI-zeolites of varying $\text{SiO}_2/\text{Al}_2\text{O}_3$ ratio and crystal size has been investigated with detailed kinetic modeling. The following conclusions could be drawn:

1. The activity of MFI zeolites for toluene ethylation is a function of concentration and strength of acid sites, highest activity was observed over MFI-80 with more strong acid sites, while para-selectivity is associated with both crystal size and $\text{SiO}_2/\text{Al}_2\text{O}_3$ ratio, displayed by MFI-2000. No catalytic activity or selectivity was observed over silicalite-1.
2. MFI-2000 yielded the highest *p*-ET selectivity (100%) due to its low-acidity and external surface area thus preventing the isomerization of *p*-ET into *m*-ET.
3. Benzene and xylenes, which are products of toluene disproportionation, were observed over MFI-80 and MFI-280 but not over MFI-2000 due to the presence of Brønsted acid sites aiding toluene disproportionation.
4. Based on Langmuir-Hinshelwood mechanism for toluene ethylation, a model with both ethanol and ethyltoluenes adsorbed on the catalyst surface sites best fits the experimental data.
5. MFI-280 required the lowest amount of activation energy to form *p*-ET which is attributed to its higher acidic content and higher activity compared with MFI-2000.

Acknowledgments

The authors are grateful to King Abdulaziz City for Science & Technology (KACST) for financial support of this research through Project No. AR-34-22. The authors also acknowledge the support from the Ministry of Higher Education, Saudi Arabia in establishing the Center of Research Excellence in Petroleum Refining & Petrochemicals at King Fahd University of Petroleum & Minerals (KFUPM). We are also grateful to Mr. Mariano Gica for the technical assistance provided during the experimental work.

References

- [1] W.W. Kaeding, L.B. Young, C.-C. Chu, J. Catal. 89 (1984) 267–273.
- [2] J. Čejka, B. Wichterlová, Catal. Rev. Sci. Eng. 44 (2002) 375–421.
- [3] S. Al-Khattaf, S.A. Ali, A.M. Aitani, N. Žilková, D. Kubicka, J. Čejka, Catal. Rev. Sci. Eng. 2014, <http://dx.doi.org/10.1080/01614940.2014.946846>.
- [4] J. Walendziewski, J. Trawczyński, Ind. Eng. Chem. Res. 35 (1996) 3356–3361.
- [5] G. Paparatto, G. De Alberti, G. Leofanti, M. Padovan, Stud. Surf. Sci. Catal. 44 (1989) 255–263.
- [6] N.E. Villareal, B.I. Kharisov, I.I. Ivanova, B.V. Romanovskii, Appl. Catal., A: Gen. 224 (2002) 161–166.
- [7] P.A. Parikh, Ind. Eng. Chem. Res. 47 (2008) 1793–1797.
- [8] C.S. Lee, T.J. Park, W.Y. Lee, Appl. Catal. 96 (1993) 151–161.
- [9] G. Paparatto, E. Moretti, G. Leofanti, F. Gatti, J. Catal. 105 (1987) 227–232.
- [10] P.A. Parikh, N. Subrahmanyam, Y.S. Bhat, A.B. Halgeri, Catal. Lett. 14 (1992) 107–213.
- [11] B. Wichterlová, J. Čejka, Catal. Lett. 16 (1992) 421–429.
- [12] Y.S. Bhat, J. Das, K.V. Rao, A.B. Halgeri, J. Catal. 159 (1996) 368–374.
- [13] T. Yashima, Y. Sakaguchi, S. Namba, Stud. Surf. Sci. Catal. 7 (1981) 739–751.
- [14] J. Nunan, J.A. Cronin, J. Cunningham, J. Am. Chem. Soc. 81 (1959) 2027–2041.
- [15] J. Čejka, A. Vondrová, B. Wichterlová, G. Vorbeck, R. Fricke, Zeolites 14 (1994) 147–153.
- [16] F. Lónyi, J. Engelhardt, D. Kalló, Zeolites 11 (1991) 169–177.
- [17] V. Bhandarkar, S. Bhatia, Zeolites 14 (1994) 39–49.
- [18] I.A. Aliev, E.I. Akhmedov, E.S. Mamedov, T.O. Gakhramanov, Petrol. Chem. 50 (2010) 373–375.
- [19] K.H. Chandavar, S.G. Hegde, S.B. Kulkarni, P. Ratnassamy, G. Chitlangia, A. Singh, A. Deo, in: D. Olson, A. Bisio (Eds.), Proceedings Sixth Int'l. Zeolite Conference, Butterworth, Guilford, 1984, pp. 325–330.
- [20] P.A. Parikh, N. Subrahmanyam, Y.S. Bhat, A.B. Halgeri, Ind. Eng. Chem. Res. 31 (1992) 1012–1016.
- [21] B.C. Lippens, J.H. de Boer, J. Catal. 4 (1965) 319–323.
- [22] N. Žilková, B. Gil, S.I. Zones, S.J. Hwang, M. Bejblová, J. Čejka, Stud. Surf. Sci. Catal. 174 (2008) 1027–1032.
- [23] N. Žilková, M. Bejblová, B. Gil, S.I. Zones, A.W. Burton, C.Y. Chen, Z. Musilova, J. Čejka, J. Catal. 266 (2009) 79–91.
- [24] H.I. de Lasa, U.S. Patent No. 5102628, 1992.
- [25] M. Osman, M.M. Hossain, S. Al-Khattaf, Ind. Eng. Chem. Res. 52 (2013) 13613–13621.
- [26] K. Toch, J.W. Thybaut, B.D. Vandegeehuove, C.S.L. Narasimhan, L. Domokos, G.B. Marin, Appl. Catal., A: Gen. 425–426 (2012) 130–144.
- [27] M.M. Hossain, L. Atanda, N. Al-Yassir, S. Al-Khattaf, Chem. Eng. J. 207–208 (2012) 308–321.
- [28] J.M. Smith, H.C. Van Ness, M.M. Abbott, Introduction to Chemical Engineering Thermodynamics, sixth ed., McGraw-Hill, Boston, MA, 2001.
- [29] S. Al-Khattaf, J.A. Atias, K. Jarosch, H. de Lasa, Chem. Eng. Sci. 57 (2002) 4909–4920.
- [30] S. Waziri, A. Aitani, S. Al-Khattaf, Ind. Eng. Chem. Res. 49 (2010) 6376–6387.
- [31] C.S. Triantafyllidis, N.P. Evmiridis, L. Nalbandian, I.A. Vasalos, Ind. Eng. Chem. Res. 38 (1999) 916–927.
- [32] M.M.J. Treacy, J.B. Higgins, R. von Ballmoos, Collection of Simulated XRD Powder Diffraction Patterns for Zeolites, fourth ed., Elsevier, London, 2001, pp. 237.
- [33] C.H. Baerlocher, W.M. Meier, D.H. Olson, Atlas of Zeolite Framework, sixth ed., Elsevier Science, Amsterdam, 2007, p 212.
- [34] T.A.J. Hardenberg, L. Mertens, P. Mesman, H.C. Muller, C.P. Nicolaides, Zeolites 12 (1992) 685–689.
- [35] N. Kadata, M. Niwa, Catal. Surv. Asia 8 (2004) 161–170.
- [36] T. Odedairo, R.J. Balasamy, S. Al-Khattaf, Ind. Eng. Chem. Res. 50 (2011) 3169–3183.
- [37] V.N. Romanikov, K.G. Ione, J. Catal. 146 (1994) 211–217.
- [38] M. Osman, L. Atanda, M.M. Hossain, S. Al-Khattaf, Chem. Eng. J. 222 (2013) 498–511.
- [39] S. Melson, F. Schutte, J. Catal. 170 (1997) 46–53.
- [40] N. Arsenova-Härtel, H. Bludau, R. Schumacher, W.O. Haag, H.G. Karge, E. Brunner, J. Catal. 191 (2000) 326–331.
- [41] D. Chen, K. Moljord, T. Fuglerud, A. Holmen, Microporous Mesoporous Mater. 29 (1999) 191–203.
- [42] N.Y. Chen, T.F. Degnan, C.M. Smith, Molecular Transport and Reaction in Zeolites: Design and Application of Shape Selective Catalysis, Wiley-VCH, Weinheim, 1994.
- [43] S. Al-Khattaf, Ind. Eng. Chem. Res. 46 (2007) 59–69.